Microemulsion Polymerization Kinetics and Mechanisms

Chorng-Shyan Chern, Hsiu-Jung Tang

Department of Chemical Engineering, National Taiwan University of Science and Technology, 43 Keelung Road, Section 4, Taipei 106, Taiwan, Republic of China

Received 22 April 2004; accepted 11 September 2004
DOI 10.1002/app.21673
Published online in Wiley InterScience (www.interscience.wiley.com).

ABSTRACT: The mechanisms of microemulsion polymerizations stabilized by sodium dodecyl sulfate in combination with pentanol were investigated with a water-insoluble dye as the probe. The major parameters chosen for study were the types of initiators [water-soluble sodium persulfate (SPS) vs oil-soluble 2,2′-azobisisobutyronitrile (AIBN)] and the polarity of the monomers [relatively hydrophobic styrene (ST) vs relatively hydrophilic methyl methacrylate (MMA)]. Both continuous particle nucleation and limited particle flocculation had a significant influence on the polymerization kinetics. For the polymerizations investigated in this work, the relatively low initiation efficiency of AIBN resulted in a reaction system showing a quite different particle nucleation mechanism than that of the ST polymerization with SPS. The formation of particle nuclei in water was suppressed to some extent, and microemulsion droplet nucleation predominated in the ST polymerization initiated by AIBN. Homogeneous nucleation played an important role, and a mixed mode of particle nucleation (microemulsion droplet nucleation and homogeneous nucleation) was operative in the MMA polymerization. The MMA polymerization experienced stronger particle flocculation than its ST counterpart.

Key words: kinetics (polym.); emulsion polymerization; particle nucleation; growth

INTRODUCTION

Microemulsion polymerization involves free-radical polymerization in a large number of monomer-swollen micelles (or microemulsion droplets, 10^0 nm in diameter).[1–18] Microemulsion droplets, stabilized by a surfactant [e.g., sodium dodecyl sulfate (SDS)] and, in some cases, a cosurfactant [e.g., pentanol (C_5OH)], form a thermodynamically stable, transparent one-phase reaction system. A typical monomer and a typical thermal initiator are styrene (ST) and sodium persulfate (SPS), respectively. The resultant latex particles (10^1 nm in diameter) contain only a few very high-molecular-weight polymer chains. Guo et al.,[3,4] Morgan et al.,[8] and Nomura and Suzuki[17] developed mechanistic models to predict the evolution of latex particles during ST microemulsion polymerization. Particle nuclei are generated via the capture of radicals by the droplets, and particle nucleation occurs throughout the polymerization.[3] Kim and Napper[19] showed that the primary particle nucleation loci are microemulsion droplets in ST polymerization, whereas the formation of particle nuclei in the aqueous phase (homogeneous nucleation)[20] plays an important role in methyl methacrylate (MMA) polymerization.

Correspondence to: C.-S. Chern (chern@ch.ntust.edu.tw).

Journal of Applied Polymer Science, Vol. 97, 2005–2013 (2005)

The feasibility of incorporating a water-insoluble dye into an extremely large number of droplets by the solubilization mechanism to study the particle nucleation and growth mechanisms in ST microemulsion polymerization has been reported in our previous work.[21–23] The water solubility of a dye (1 ppm) is two orders of magnitude smaller than that of ST. Under the circumstances, dye molecules can be incorporated into latex particles only when radicals enter the droplets and the subsequent polymerization occurring therein successfully converts them into particle nuclei. On the contrary, primary particles nucleated in the aqueous phase should not contain any dye because of the greatly retarded transport of dye molecules from microemulsion droplets or latex particles, across the aqueous phase, and then into latex particles originating from homogeneous nucleation. The insignificant mass transfer of the blue dye from the aqueous phase to the latex particles has been demonstrated in our previous work.[24] Thus, the weight percentage of the dye incorporated into the latex particles (P_{dye}) serves as an indicator of the extent of microemulsion droplet nucleation. At a constant monomer conversion (X), P_{dye} decreases with an increasing initial initiator concentration ($[I]_0$).[23] This has been attributed to the increased probability of particle formation in the aqueous phase with $[I]_0$. To gain a better understanding of the particle nucleation and growth mechanisms, we investigated microemulsion polymerizations with different initiators [water-soluble SPS vs oil-soluble 2,2′-azobisisobutyronitrile (AIBN)] and monomers (rela-

tively hydrophobic ST vs relatively hydrophilic MMA) with the dye technique in this work. The AIBN-initiated ST microemulsion polymerization was expected to show an insignificant formation of particle nuclei in the aqueous phase, in contrast to the SPS-initiated polymerization. In comparison with the ST polymerization, homogeneous nucleation was anticipated to be greatly enhanced in the MMA microemulsion polymerization initiated by SPS.

EXPERIMENTAL

Materials

The chemicals used in this work included ST (Taiwan Styrene Co., Kaohsiung, Taiwan), MMA (Kaohsiung Monomer Co., Kaohsiung, Taiwan), SDS (J.T. Baker, Phillipsburg, NJ), methanol (Acros, Fair Lawn, NJ), C_5OH (Janssen Chimica, Geel, Belgium), SPS (Riedel-de Haen), AIBN (Showa, Osaka, Japan), sodium bicarbonate (Riedel-de Haen, Hanover, Germany), tris(hydroxymethyl)aminomethane (Acros), a water-insoluble dye (Blue 70; Shenq-Fong Fine Chemical, Ltd., China), hydroquinone (Nacalai Tesque, Kyoto, Japan), polystyrene (PST; average molecular weight = 2.5×10^5; Acros), a series of PST standards for gel permeation chromatography (GPC) calibration (Thomsen Instrument, Oceanside, CA), tetrahydrofuran (THF; J.T. Baker), toluene (Acros), nitrogen (Ching-Feng-Harng Co., Taipei, Taiwan), and deionized water (Nanopure ultrapure water system, Barnsted (Dubuque, IA); specific conductance < 0.057 μS/cm). ST and MMA were distilled under reduced pressure, and AIBN was purified by crystallization from dry methanol before use. All other chemicals were used as received.

Microemulsion polymerization and characterization

The ST microemulsion was prepared according to Guo and coworkers.[2–4] Batch polymerization was carried out at 70 ± 0.5°C in a 500-mL reactor equipped with a four-bladed fan turbine agitator, a thermometer, and a reflux condenser. Before the polymerization was begun, the reaction medium was purged by N_2 for 30 min to remove the dissolved oxygen. Latex samples, stopped short of complete conversion by a small amount of hydroquinone, were taken during the polymerization for the kinetic study. The final latex product was filtered through a 325-mesh screen to collect the filterable solids. X was determined by a gravimetric method. Transmission electron microscopy (TEM-1200 EXII, JEOL, Tokyo, Japan) was used to determine the weight-average latex particle diameter (d_w) and the polydispersity index of the particle size distribution [PDI(PSD) = d_w/d_n, where d_n is the number-average particle diameter]. The number of latex particles per unit volume of water (N_p) was calculated as follows:

$$N_p = W_{ST}X/[(\pi/6)d_w^3\,\rho_{PST}W_w] \quad (1)$$

where W_{ST} is the initial weight of ST, ρ_{PST} is the density of PST, and W_w is the total weight of water.

The zeta potential (ζ) of latex particles was measured with a Malvern Zetamaster (Worcestershire, UK). A buffer solution of 20 mM tris(hydroxymethyl)-aminomethane (pH 7) was used as the dilution solution for the latex sample (latex/buffer = 1/20 v/v). The reported ζ value represents an average of at least five measurements. Latex particles were precipitated with an excess of methanol, and this was followed by thorough washing with methanol and water for the removal of residual SDS, C_5OH, and other impurities. The weight-average molecular weight (M_w) and polydispersity index of the molecular weight distribution [PDI(MWD) = M_w/M_n, where M_n is the number-average molecular weight] of PST [or poly(methyl methacrylate) (PMMA)] was determined by GPC (515/2410/Styragel HR2, HR4, and HR6, Waters, Milford, MA) calibrated by a series of PST standards.

To determine the amount of dye incorporated into the latex particles during the polymerization, we allowed the latex sample to stand at room temperature over 15 days. In this manner, a thin layer of a blue precipitate (originating from the bulk dye suspended in the sample) was observed on the bottom of the sample. The sample, consisting of latex and methanol (latex/methanol = 3/7 w/w) was mixed thoroughly for 30 s to precipitate latex particles. This was followed by centrifugation (J2-21, Beckman, Fullerton, CA), the removal of the supernatant, and the addition of fresh methanol. This process was repeated five times to further remove the dye molecules that were not incorporated into latex particles, SDS, C_5OH, and residual ST and SPS. Increasing the number of cycles did not change the value of P_{dye} to any appreciable extent. The precipitated polymer was then placed in a vacuum oven at 50°C over 24 h. Approximately 0.25 g of the dried polymer was dissolved in 10 mL of THF for the determination of P_{dye} according to the calibration curve with an extinction coefficient of 7.313×10^4 mL/cm g established by UV absorbance at 678 nm (UV-160A, Shimadzu, Sydney, Australia). Because SDS and C_5OH may not have been removed completely from the sample, standard solutions of PST (Acros) in 10 mL of THF (2×10^{-4}–1.2×10^{-3} g/mL) were used to construct a calibration curve with an extinction coefficient of 2.299×10^3 mL/cm g. The actual amount of PST in the sample necessary for the calculation of P_{dye} was determined accordingly. For the MMA polymerization, PMMA, used to construct the calibration curve by UV absorbance at 240 nm, was prepared by the solution polymerization of 180 g of

toluene, 20 g of MMA, and 0.4 g of AIBN at 70°C over 6 h in our laboratory. The reported P_{dye} value represents an average of at least two measurements. The reproducibility of the P_{dye} data is reasonably good.

RESULTS AND DISCUSSION

Effect of the type of initiator (SPS vs AIBN)

The recipe for the ST polymerization at 70°C consisted of 250 g of water, 27.5 g (381.4 m*M*) of SDS, 12.0 g (544.5 m*M*) of C_5OH, 14.8 g (576.9 m*M*) of ST, a water-insoluble dye (0.15 wt % based on total monomer), 0.75 m*M* SPS (or 5.49 m*M* AIBN), and 0.1 m*M* sodium bicarbonate (buffer), for which the molar concentration was based on the total water. The levels of SPS and AIBN were chosen in such a way that both runs showed comparable rates of polymerization, $R_p = [M]_0 dX/dt$, where $[M]_0$ is the initial monomer concentration, t is the reaction time, and dX/dt is the least-squares best fitted slope of the linear portion of the X–t data ($X = 10$–60%), which are not shown here. The values of R_p (mol/L min) obtained from the polymerizations with SPS and AIBN were 4.37×10^{-2} and 5.03×10^{-2}, respectively. The AIBN concentration required to match the SPS-initiated polymerization kinetics was very high.

Under the assumption that (1) all the radicals generated in the aqueous phase enter the droplets and initiate the polymerization therein, (2) the bimolecular termination reaction in the aqueous phase is negligible, (3) the entry of radicals into latex particles is insignificant, and (4) the growing polymer chain in a particle is primarily terminated by the chain-transfer reaction, the following equation was developed to predict the reaction kinetics:[8,17]

$$\ln(1 - X) = -fk_d[I]_0 k_p[M]_{d,0} t^2/[M]_0 \qquad (2)$$

where f is the initiator efficiency factor, k_d is the initiator decomposition rate constant, k_p is the propagation rate constant, and $[M]_{d,0}$ is the initial monomer concentration in the droplets. The first assumption implies a polymerization system with $f = 1$. The relationships $R_p = k_p[M]_p N_1$ and $N_1 = 2fk_d[I]_0 N_A t$ were used in the development of eq. (2), where $[M]_p$ is the ST concentration in the particle, N_A is Avogadro's number, and N_1 is the number of particles containing one radical produced via the capture of radicals by droplets. The value of f is regarded as approximately constant (0.5–0.8), depending on the viscosity of the reaction medium. Thus, the actual R_p value should be lower than that predicted by eq. (2). Kuo et al.[1] showed that the limited flocculation of particle nuclei has a significant influence on the reaction kinetics. The limited particle flocculation is characterized by the progressively increasing colloidal stability of the flocculated particle nuclei accompanied by a reduced total particle surface area (i.e., the increased particle surface charge density). Such a phenomenon would have an effect on N_1. This is because the bimolecular termination of radicals belonging to two particles may occur upon flocculation and result in the reduction of N_1. On the contrary, N_1 does not vary to any extent if the flocculation process involves (1) two particles containing no radicals or (2) one particle containing one radical and the other containing no radicals. In this study, an empirical parameter F, which took into account the limited particle flocculation, was incorporated into eq. (2), as shown in the following equation:

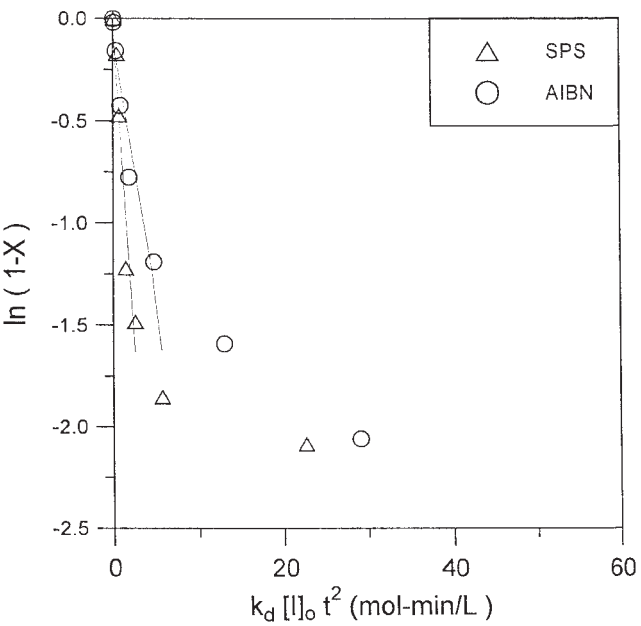

Figure 1 Plot of $\ln(1 - X)$ versus $k_d[I]_0 t^2$ for ST microemulsion polymerizations at 70°C with different initiators: (△) 0.75 m*M* SPS and (○) 5.49 m*M* AIBN. The straight lines represent the least-squares best fitted results (coefficient of determination = 0.92 for both runs).

$$\ln(1 - X) = -Ffk_d[I]_0 k_p[M]_{d,0} t^2/[M]_0 \qquad (3)$$

The smaller F is, the stronger the limited particle flocculation is (i.e., the smaller N_1 is). On the other hand, the effect of the limited particle flocculation is negligible when F is equal to 1.

According to eq. (3), plotting the $\ln(1 - X)$–$k_d[I]_0 t^2$ data should result in a straight line with a slope of $[-Ffk_p[M]_{d,0}/[M]_0]$. The expressions used to calculate k_d (1/min) were $3.64 \times 10^{16}\exp(-33{,}500/RT)$ and $9.48 \times 10^{16}\exp(-30{,}775/RT)$ for SPS[25] and AIBN,[26] respectively, where R is the gas constant and T is the absolute temperature. Figure 1 shows that this model predicted the reaction kinetics reasonably well up to $X = 70$–80% [i.e., $\ln(1 - X) = -1.2$ to -1.9]. The poor performance of eq. (3) in the high-conversion region

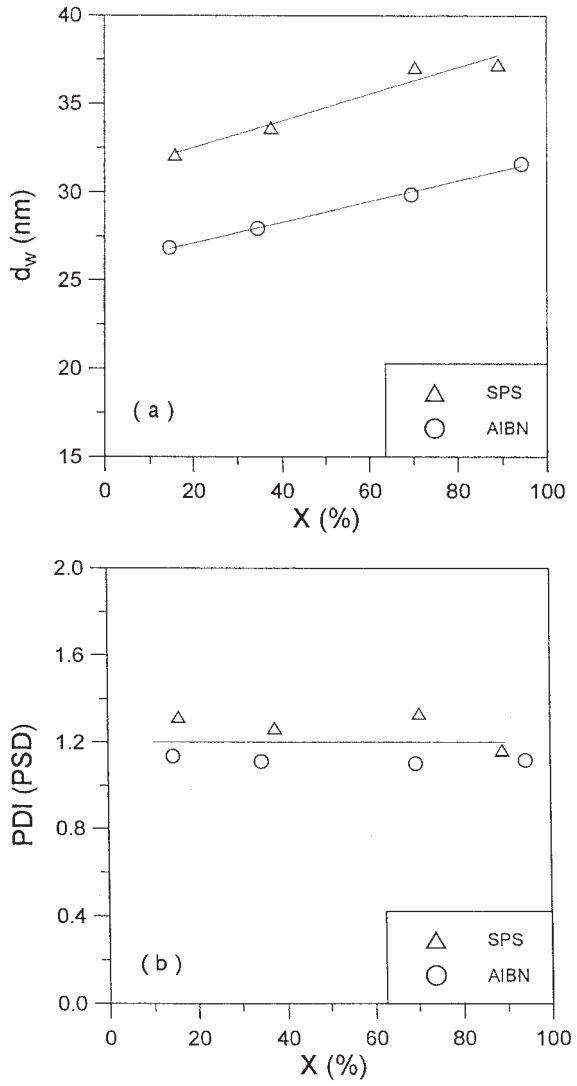

Figure 2 (a) d_w and (b) PDI(PSD) as functions of X for ST microemulsion polymerizations at 70°C with different initiators: (△) 0.75 mM SPS and (○) 5.49 mM AIBN.

was attributed to the bimolecular termination and diffusion-controlled propagation reactions.[12] The slopes of the least-squares best fitted straight lines in Figure 1 are −0.63 and −0.25 L/mol min for the SPS- and AIBN-initiated polymerizations, respectively. With $f = 1$, $k_p = 1.44 \times 10^{10} \exp(-8958.4/RT)$ L/mol min,[26] $[M]_{d,0} = 7$ mol/L,[3] and $[M]_0 = 0.577$ mol/L, the values of F were estimated to be 1.85×10^{-6} and 7.45×10^{-7} for the SPS- and AIBN-initiated polymerizations, respectively. Indeed, limited particle flocculation plays an important role in the ST microemulsion polymerization with SDS and C_5OH as the stabilizing reagents. The distinguishable kinetic data between the SPS- and AIBN-initiated polymerizations in Figure 1 reflect the fact that the Morgan–Nomura model is not applicable to polymerizations initiated by AIBN. This is simply because the model does not consider the partitioning of AIBN between the monomer phase and the aqueous phase. Under the circumstances, whether the limited particle flocculation has an influence on the AIBN-initiated polymerization is inconclusive.

Figure 2 shows d_w and PDI(PSD) (or d_w/d_n) with the progress of polymerization. At a constant value of X, both d_w and PDI(PSD) obtained from the AIBN-initiated polymerization were smaller than those obtained from the SPS counterpart. Figure 3 shows N_p and P_{dye} as functions of X. Very different P_{dye}–X profiles for the AIBN- and SPS-initiated polymerizations can be observed. P_{dye} increased with increasing X in the SPS-initiated polymerization, whereas it remained relatively constant with the progress of the AIBN-initiated polymerization. All these data suggest that SPS- and AIBN-initiated polymerizations have different particle nucleation mechanisms, and this is also reflected in the different values of F. The generation rate of SPS

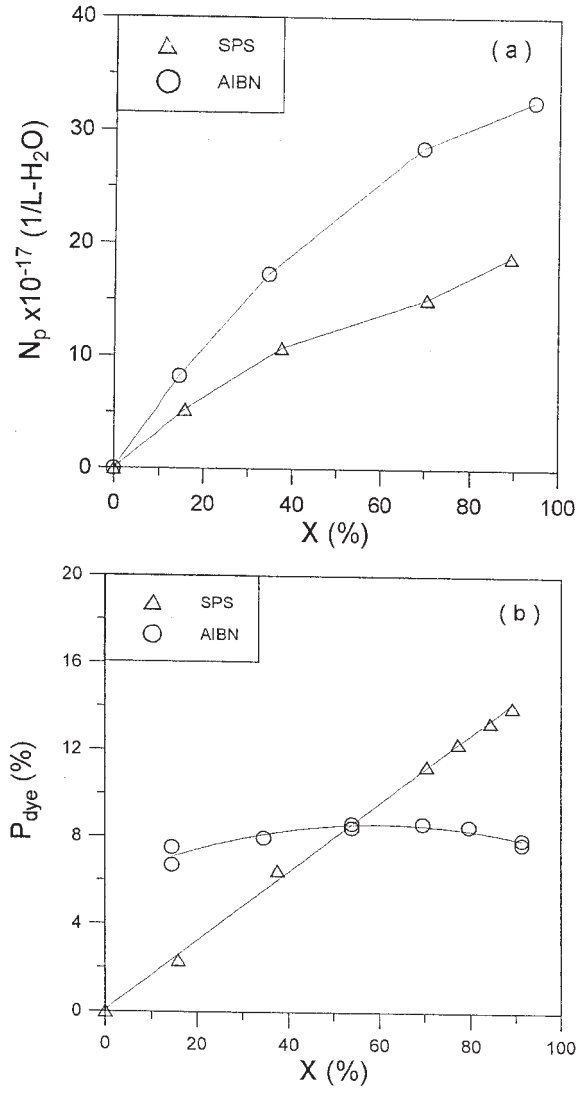

Figure 3 (a) N_p and (b) P_{dye} as functions of X for ST microemulsion polymerizations at 70°C with different initiators: (△) 0.75 mM SPS and (○) 5.49 mM AIBN.

radicals (SO_4^{-}*) in the aqueous phase at 70°C ($2fk_d[I]_0$) is 1.47×10^{18} 1/L min. The water solubility of AIBN is 4×10^{-5} g/g of H_2O,[27] and the partitioning of AIBN between the monomer phase and the water phase is 115/1.[28] Under the assumption that f is equal to 1, the generation rates of AIBN radicals [$(CH_3)_2(CN)C$*] in the monomer phase and in the aqueous phase at 70°C are 1.61×10^{19} and 1.40×10^{17} 1/L min, respectively. The concentration of AIBN radicals generated in the aqueous phase is two orders of magnitude smaller than that in the monomer phase. This suggests that the formation of particle nuclei in the aqueous phase should be rather limited. Considering the limiting case in which AIBN radicals generated in the droplets predominated in the particle nucleation process, we find that P_{dye} obtained from the AIBN-initiated polymerization should be much larger than that obtained from the SPS counterpart. However, this is not the case, as shown in Figure 3(b).

The increased N_p and P_{dye} values with X can be attributed to the continuous particle nucleation via the capture of the water-borne radicals by droplets in the SPS-initiated polymerization (Fig. 3). This is because the ratio of the number of the final particles to that of the initial droplets is very small (10^{-3}),[2–4] and this implies that the probability of radicals entering the particles is insignificant in comparison with the very large population of droplets. The propagation reaction of radicals with monomer inside these particles itself is not sufficient to attain the particle growth rate, and so the limited particle flocculation must contribute significantly to the final particle dimension. As a result, F is much smaller than 1. Furthermore, droplets that do not participate in the particle formation process only serve as a reservoir to supply the growing particles with monomer. In the absence of droplet nucleation, the transport of the monomer from droplets to particles and the subsequent polymerization of the monomer supplies therein do not increase the dye content in the particles but increase the polymer weight instead. This then leads to a reduction in P_{dye}, but this dilution effect cannot be important in the SPS-initiated polymerization because of the increased P_{dye} value with X [Fig. 3(b)]. The values of F and the N_p and P_{dye} data in Figure 3 strongly suggest that the SPS-initiated polymerization kinetics is primarily controlled by the continuous particle nucleation and limited particle flocculation mechanisms.

The increased N_p value with X demonstrates the important role of the continuous particle nucleation in the AIBN-initiated polymerization [Fig. 3(a)]. P_{dye} remains relatively constant [Fig. 3(b)] even though particle nuclei that are most likely produced by droplet nucleation form throughout the polymerization. This is probably due to the delicate balance between the slow droplet nucleation and the diffusion of the monomer from droplets to particles, followed by the consumption of the monomer supplies therein. On the basis of the recipes (83.57 mM AIBN on the basis of total ST vs 0.75 mM SPS on the basis of total water) and the dramatically different natures of the initiators used in this work, the termination reaction between the neighboring AIBN radicals generated in pairs within the extremely small droplets is more important than the polymerization initiated by SPS radicals generated in the aqueous phase. It can then be postulated that the particle nucleation process involves (1) the desorption of one radical out of the droplet containing two AIBN radicals, followed by the propagation reaction of the remaining radical with the monomer, (2) the entry of one radical into the droplet containing two AIBN radicals, followed by the bimolecular termination and the subsequent propagation reaction of the survivor with the monomer, or (3) the entry of one radical into the droplet containing no radicals, followed by the propagation reaction of this radical with the monomer therein. Such a particle nucleation mechanism would be characterized by a relatively low initiation efficiency ($f < 1$). Another contributing factor is that AIBN radicals are more hydrophilic than AIBN molecules. Therefore, AIBN radicals could experience the desorption–absorption process frequently in a very short period of time. A much higher AIBN concentration is thus required to give a value of R_p comparable to that of the SPS counterpart. Moreover, the inefficient initiation reaction makes the effects of the absorption and consumption of the monomer supplies by the existing particles more competitive. As a result of the counterbalance of these two opposite effects, P_{dye} remains relatively constant during polymerization. Nevertheless, there is no doubt about the very important role of droplet nucleation in the AIBN-initiated polymerization, especially during the first half of the reaction [Fig. 3(b)]. To estimate the magnitude of f in the AIBN-initiated polymerization, we assume that the SPS- and AIBN-initiated polymerizations experience similar extents of particle flocculation. This assumption is reasonable because both runs show comparable changes in the particle volume during polymerization $\{1 - [d_w(0.89)/d_w(0.16)]^3 = 0.56$ for the SPS-initiated polymerization and $1 - [d_w(0.94)/d_w(0.15)]^3 = 0.63$ for the AIBN-initiated polymerization, where the numeric values in parentheses represent the fractional monomer conversions; Fig. 2(a)$\}$. The larger the change is in the particle volume, the stronger the limited particle flocculation is. Thus, the value of f for the AIBN-initiated polymerization is estimated to be 0.4 [$F(SPS)/F(AIBN) = 7.45 \times 10^{-7}/1.86 \times 10^{-6}$] as long as f is 1 for the SPS-initiated polymerization.

Although the data are quite scattered, ζ of particles obtained from the SPS- and AIBN-initiated polymerizations seems to decrease to a minimum and then increase toward the end of polymerization (Fig. 4).

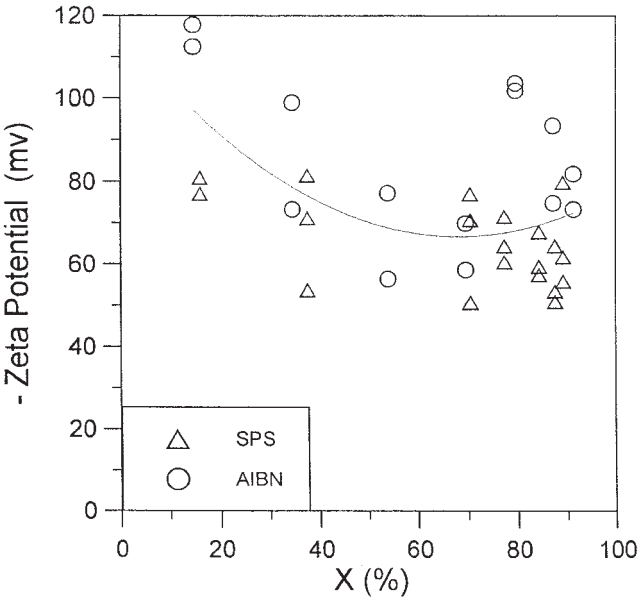

Figure 4 ζ of latex particles as a function of X for ST microemulsion polymerizations at 70°C with different initiators: (△) 0.75 mM SPS and (○) 5.49 mM AIBN.

The decreased ζ value with X is primarily due to the expanding particle–water interfacial area. Co et al.[11] showed that the number density of micelles increases, whereas the size of micelles decreases, during ST microemulsion polymerization. ζ (i.e., the surface charge density) may thus decrease with increasing X if the structure of the micelles is quite compact and the disbanded rate of micelles is not fast enough to allow SDS molecules to diffuse across the aqueous phase and then adsorb onto the particle surfaces. Beyond the minimum, the increased ζ value with X can be attributed to the limited particle flocculation, which greatly reduces the total particle surface area. Another contributing factor is the accelerated disbanded rate of micelles to supply the particle surfaces with SDS. As more SDS molecules are transported from micelles to particles, it is more difficult to maintain the integrity of these shrinking micelles during the latter stage of polymerization. Therefore, the growing particles can acquire SDS molecules more easily, and this leads to a higher particle surface charge density.

M_w obtained from the AIBN-initiated polymerization is much smaller than that obtained from the SPS counterpart [Fig. 5(a)]. The PDI(MWD) data are centered around 1.4 for both the SPS- and AIBN-initiated polymerizations [Fig. 5(b)]. Furthermore, both M_w and PDI(MWD) are relatively insensitive to changes in X. The deviations in both M_w and PDI(MWD) between this work and theoretical predictions [$M_w = 2 \times 10^6$ g/mol[29] and PDI(MWD) = 2 for the chain-transfer-reaction-limited ST polymerization[17]] are due to the fact that the bimolecular termination of radicals belonging to two particles might take place upon limited particle flocculation. This would then shortstop these encountered radicals before the chain-transfer reaction could happen. The final average number of PST chains per particle (N_c) can be estimated as follows:

$$N_c = (\pi/6) d_w^3 \rho_{PST} N_A / M_w \quad (4)$$

The values of N_c are 12.2 and 22.7 for the SPS- and AIBN-initiated polymerizations, respectively. These values are larger than those expected for the ST microemulsion polymerizations (only a few PST chains per particle).[2–4] This is also reflected in the relatively large volume ratio of the final particles to the initial droplets, $(d_{w,f}/d_{d,0})^3 \approx (40/4)^3 = 10^3$, where $d_{w,f}$ and $d_{d,0}$ are the final particle diameter and initial droplet diameter,[30] respectively. Mass balance indicates that such a 1000-fold increase in the particle volume cannot

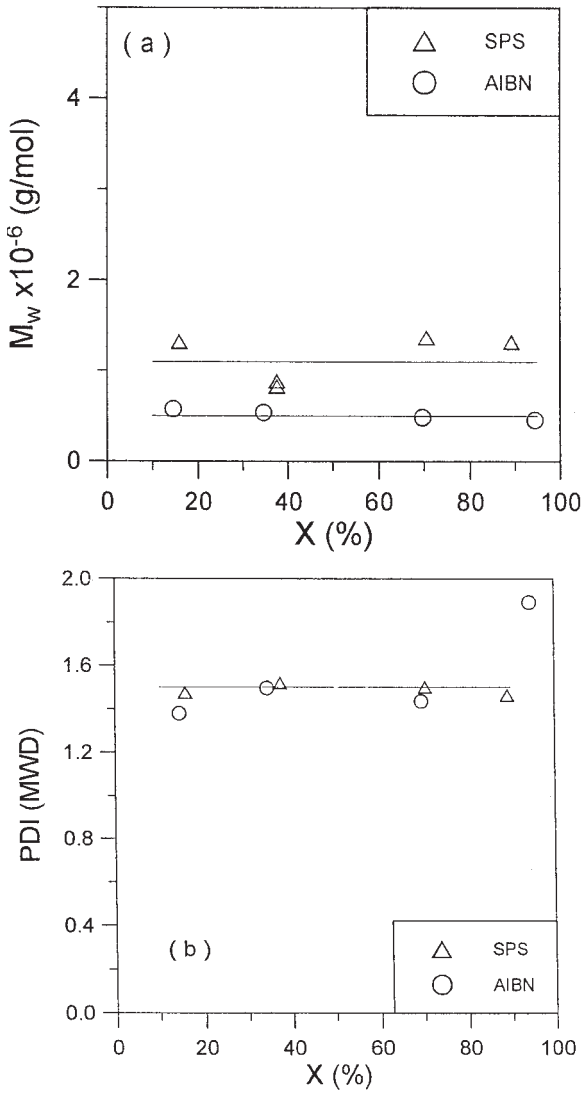

Figure 5 (a) M_w and (b) PDI(MWD) as functions of X for ST microemulsion polymerizations at 70°C with different initiators: (△) 0.75 mM SPS and (○) 5.49 mM AIBN.

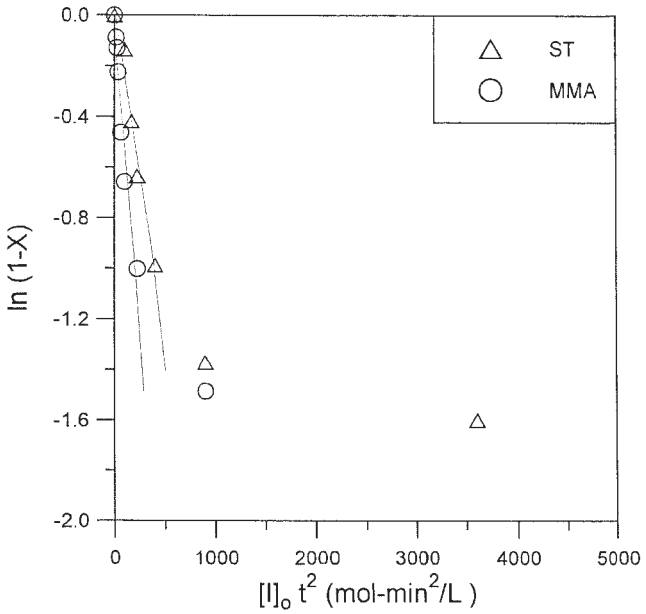

Figure 6 Plot of ln $(1 - X)$ versus $[I]_0t^2$ for SPS-initiated microemulsion polymerizations of ST or MMA at 70°C: (△) ST and (○) MMA. The straight lines represent the least-squares best fitted results (coefficient of determination = 0.97 and 0.94 for ST and MMA polymerizations, respectively).

be achieved by the propagation reaction of radicals with the monomer inside the particles alone. All these data support the postulation that limited particle flocculation occurs in ST microemulsion polymerizations stabilized by SDS and C_5OH and initiated by SPS (or AIBN).

Effect of the type of monomer (ST vs MMA)

The recipe for the polymerizations at 70°C consisted of 250 g of water, 27.5 g (381.4 m*M*) of SDS, 12.0 g (544.5 m*M*) of C_5OH, 576.9 m*M* ST (or MMA), a water-insoluble dye (0.15 wt % based on the total monomer), 0.5 m*M* SPS, and 0.1 m*M* sodium bicarbonate. Figure 6 shows the $\ln(1 - X)$–$[I]_0t^2$ data, and the slopes of the least-squares best fitted straight lines are -2.6×10^{-3} and -4.5×10^{-3} L/mol min^2 for the ST and MMA polymerizations, respectively. With $k_p = 9.72 \times 10^8 \exp(-6955/RT)$ L/mol min for MMA[31] and the assumption that the ST and MMA polymerizations have comparable values of $[M]_{d,0}$, the ratio of F(MMA) to F(ST) can be estimated to be 1.36/1. This implies that the MMA polymerization experiences stronger particle flocculation than the ST counterpart. This results in a smaller population of particles with a larger particle size. This is further supported by the data of d_w and N_p in Figures 7(a) and 8(a), respectively. The values of $(d_{w,f}/d_{d,0})^3$ are about $(41/4)^3 = 1077$ and $(50/4)^3 = 1953$ for the ST and MMA polymerizations, respectively. The ST and MMA polymerizations show comparable values of R_p [$(2.93 \pm 0.09) \times 10^{-2}$ mol/L min], and this indicates the more pronounced particle flocculation experienced in the MMA polymerization to achieve the larger volume ratio of the final particles to the initial droplets. The initial MMA droplet diameter is assumed to be 4 nm in the aforementioned calculation. In addition, the PDI(PSD) data obtained from the ST and AIBN polymerizations almost fall in a single straight line [Fig. 7(b)]. On the basis of the data presented here, both the continuous particle nucleation and limited particle flocculation mechanisms operate in the MMA polymerization.

The P_{dye}–X data in Figure 8(b) strongly suggest that homogeneous nucleation is more important in the MMA polymerization. This is consistent with the work of Kim and Napper.[19] A mixed mode of particle nucleation (droplet nucleation and homogeneous nu-

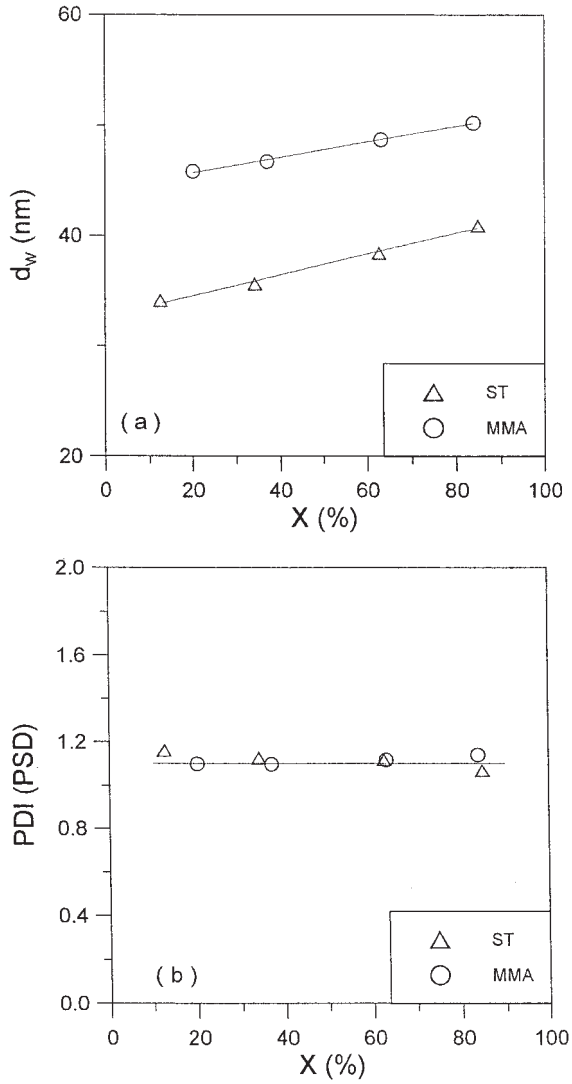

Figure 7 (a) d_w and (b) PDI(PSD) as functions of X for ST and MMA microemulsion polymerizations at 70°C: (△) ST and (○) MMA.

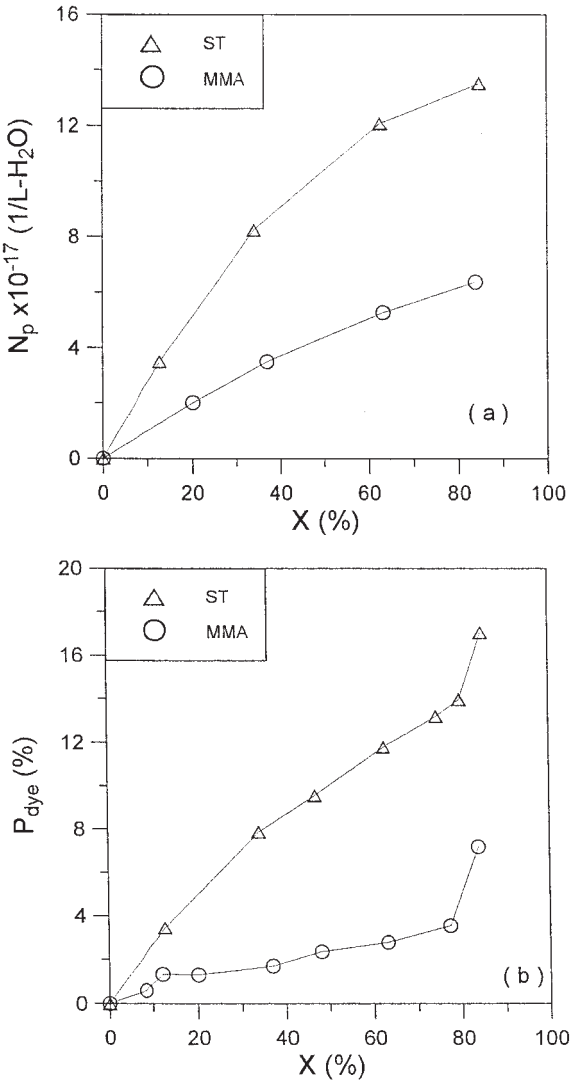

Figure 8 (a) N_p and (b) P_{dye} as functions of X for ST and MMA microemulsion polymerizations at 70°C: (△) ST and (○) MMA.

cleation) governs the evolution of PMMA particles during polymerization. It is postulated that the major part of C_5OH is present within the droplet surface layer and the particle nuclei generated in the aqueous phase may carry very few C_5OH molecules on their surfaces; this leads to the decreased colloidal stability. This is because the incorporation of amphipathic C_5OH into the adsorbed layer of SDS around a particle can greatly reduce the electrostatic repulsion force between two anionic SDS molecules, minimize the oil–water interfacial tension, and hence enhance the colloidal stability. Another contributing factor is that the surface coverage of the relatively hydrophilic PMMA particles by SDS/C_5OH is lower than that of the ST counterpart. Therefore, the relatively unstable PMMA particles, especially those nucleated in the aqueous phase, show a greater tendency to flocculate with one another to reduce the total particle surface area, increase the particle surface charge density, and, consequently, regain satisfactory colloidal stability during polymerization.

Figure 9 shows that ζ gradually increases with increasing X in the MMA polymerization, whereas it decreases to a minimum and then goes up toward the end of the ST polymerization. In comparison with the ST counterpart, ζ is much lower (i.e., the colloidal system is less stable), and so the limited particle flocculation is much stronger during the early stage of the MMA polymerization. The ST and MMA polymerizations eventually exhibit comparable values of ζ to achieve adequate colloidal stability during the second half of polymerization. At a constant value of X, M_w of PMMA is lower than that of PST as a result of the significant formation of particle nuclei in the aqueous phase and limited particle flocculation (Fig. 10).

CONCLUSIONS

Both continuous particle nucleation and limited particle flocculation have a significant influence on the polymerization kinetics when the reaction system is stabilized by SDS and C_5OH. In comparison with the ST polymerization with water-soluble SPS as the initiator, a much higher level of oil-soluble AIBN is required to attain a comparable R_p value because of its relatively low initiation efficiency. This characteristic of AIBN makes the reaction system show a quite different particle nucleation mechanism than that of the SPS-initiated polymerization. The dye content data indicate that the probability for particle nuclei to form in the aqueous phase is rather slim, and droplet nu-

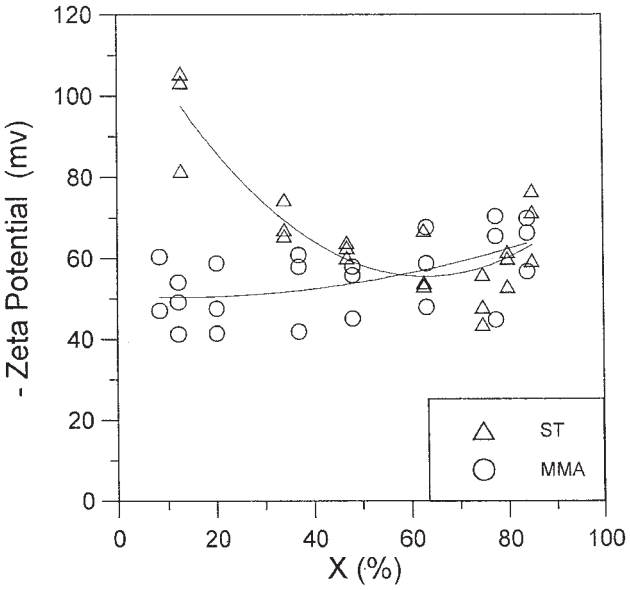

Figure 9 ζ of latex particles as functions of X for ST and MMA microemulsion polymerizations at 70°C: (△) ST and (○) MMA.

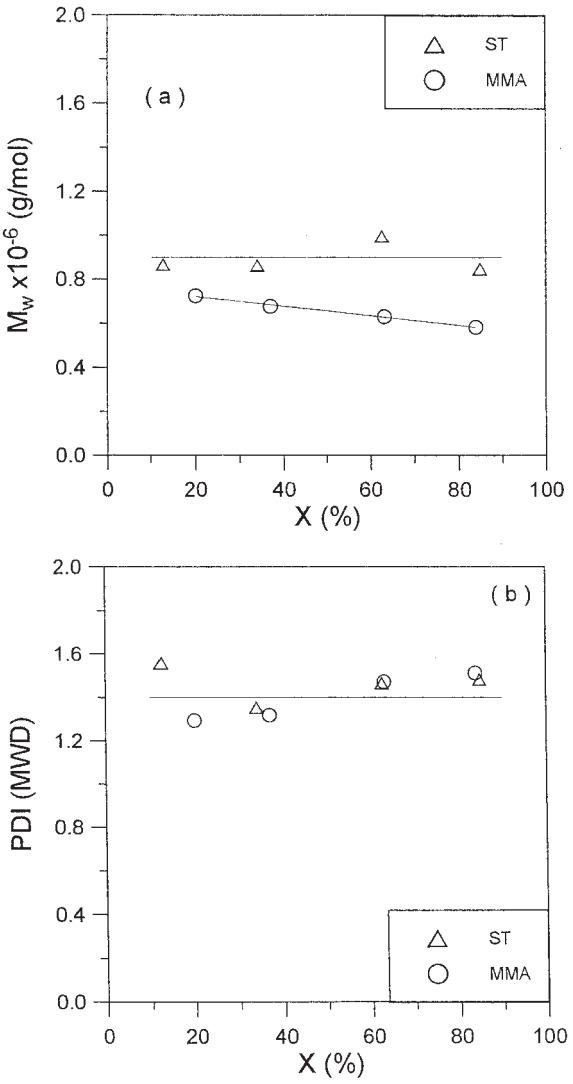

Figure 10 (a) M_w and (b) PDI(MWD) as functions of X for ST and MMA microemulsion polymerizations at 70°C: (△) ST and (○) MMA.

cleation predominates in the ST polymerization initiated by AIBN. However, homogeneous nucleation cannot be ruled out when SPS is used as the initiator in the ST polymerization.

The effect of monomers with different water solubilities (i.e., relatively hydrophobic ST versus relatively hydrophilic MMA) is dramatic. Nucleation taking place in the aqueous phase plays an important role, and a mixed mode of particle nucleation (droplet nucleation and homogeneous nucleation) is operative in the MMA polymerization. The limited particle flocculation is stronger in the MMA polymerization than in the ST counterpart. This is closely related to the difference in the surface coverage with SDS and C_5OH between the PMMA and PST particles during polymerization. The PMMA particles with a lower surface charge density show a greater tendency to flocculate with one another to reduce the total particle surface area and enhance the colloidal stability.

References

1. Kuo, P. L.; Turro, N. J.; Tseng, C. M.; El-Aasser, M. S.; Vanderhoff, J. W. Macromolecules 1987, 20, 1216.
2. Guo, J. S.; El-Aasser, M. S.; Vanderhoff, J. W. J Polym Sci Part A: Polym Chem 1989, 27, 691.
3. Guo, J. S.; Sudol, E. D.; Vanderhoff, J. W.; El-Aasser, M. S. J Polym Sci Part A: Polym Chem 1992, 30, 691.
4. Guo, J. S.; Sudol, E. D.; Vanderhoff, J. W.; El-Aasser, M. S. J Polym Sci Part A: Polym Chem 1992, 30, 703.
5. Perez-Luna, V. H.; Puig, J. E.; Castano, V. M.; Rodriguez, B. E.; Murthy, A. K.; Kaler, E. W. Langmuir 1990, 6, 1040.
6. Puig, J. E.; Perez-Luna, V. H.; Perez-Gonzalez, M.; Macias, E. R.; Rodriguez, B. E.; Kaler, E. W. Colloid Polym Sci 1993, 271, 114.
7. Full, A. P.; Kaler, E. W.; Arellano, J.; Puig, J. E. Macromolecules 1996, 29, 2764.
8. Morgan, J. D.; Lusvardi, K. M.; Kaler, E. W. Macromolecules 1997, 30, 1897.
9. Morgan, J. D.; Kaler, E. W. Macromolecules 1998, 31, 3197.
10. Co, C. C.; Kaler, E. W. Macromolecules 1998, 31, 3203.
11. Co, C. C.; de Vries, R.; Kaler, E. W. Macromolecules 2001, 34, 3224.
12. de Vries, R.; Co, C. C.; Kaler, E. W. Macromolecules 2001, 34, 3233.
13. Co, C. C.; Cotts, P.; Burauer, S.; de Vries, R.; Kaler, E. W. Macromolecules 2001, 34, 3245.
14. Antonietti, M.; Bremser, W.; Muschenborn, D.; Rosenauer, C.; Schupp, B.; Schmidt, M. Macromolecules 1991, 24, 6636.
15. Antonietti, M.; Basten, R.; Rohmann, S. Macromol Chem Phys 1995, 196, 441.
16. Gan, L. M.; Chew, C. H.; Lee, K. C.; Ng, S. C. Polymer 1994, 35, 2659.
17. Nomura, M.; Suzuki, K. Macromol Chem Phys 1997, 198, 3025.
18. Suzuki, K.; Nomura, M.; Harada, M. Colloids Surf A 1999, 153, 23.
19. Kim, D. R.; Napper, D. H. Macromol Rapid Commun 1996, 17, 845.
20. Fitch, R. M. Br Polym J 1973, 5, 467.
21. Chern, C. S.; Wu, L. J. J Polym Sci Part A: Polym Chem 2001, 39, 898.
22. Chern, C. S.; Wu, L. J. J Polym Sci Part A: Polym Chem 2001, 39, 3199.
23. Chern, C. S.; Tang, H. J. Polym React Eng 2003, 11, 213.
24. Chern, C. S.; Chen, T. J.; Liou, Y. C. Polymer 1998, 39, 3767.
25. Kolthoff, I. M.; Miller, I. K. J Am Chem Soc 1951, 73, 3055.
26. Brandrup, J.; Immergut, E. H. Polymer Handbook, 3rd ed.; Wiley: New York, 1989; Chapter 2, pp 3 and 76.
27. Alduncin, J. A.; Forcada, J.; Asua, J. M. Macromolecules 1994, 27, 2256.
28. Nomura, M.; Ikoma, J.; Fujita, K. J Polym Sci Part A: Polym Chem 1993, 31, 2103.
29. Kukulj, D.; Davis, T. P.; Gilbert, R. G. Macromolecules 1998, 31, 994.
30. Guo, J. S.; El-Aasser, M. S.; Sudol, E. D.; Yue, H. J.; Vanderhoff, J. W. J Colloid Interface Sci 1990, 140, 175.
31. Soh, S. K. J Appl Polym Sci 1980, 25, 2993.